THE ROLES OF FREQUENCY AND APERTURE IN LINAC ACCELERATOR DESIGN*

Z. D. FARKAS
Stanford Linear Accelerator Center, Stanford University, Stanford, CA 94309

ABSTRACT

Expressions for accelerating structure parameters, including those that determine the peak and average power inputs required to attain a given gradient, are given as functions of aperture to wavelength ratio for a $2\pi/3$ mode disk-loaded guide. The value of the wavelength to aperture ratio varies over a large range, corresponding to group velocities that vary from nearly zero to nearly the speed of light. The parameters exhibit proper asymptotic behavior in both limits. These parameters are benchmark values to which parameters for other modes and for other structure shapes can be compared. For example, it will be shown that the increased peak surface field to accelerating field ratio due to increased aperture to wavelength ratio can be reduced by shaping the iris profile. Structure shapes are varied not only to show possible improvement of structure parameters, but also to improve ease of mechanical fabrication and temperature control.

ACCELERATING STRUCTURE LOCAL PARAMETERS

In this section the local accelerating structure parmeters are defined and then expressed in terms of aperture to wavelength ratio, $a_\lambda \equiv a/\lambda$: Assume a SLAC-type $2\pi/3$ mode disk-loaded structure with an aperture a, cavity radius b at operating wavelength λ. Define the structure parameters that depend only on a_λ:

$$\beta_g = \frac{v_g}{c} = \frac{P_t/w}{c}\ , \qquad b_a = \frac{b}{a}\ , \qquad E_{rl} = \frac{E_p}{E}\ . \tag{1}$$

Here v_g is the group velocity, P_t the power flow, w the energy stored per unit length, E_p the local peak surface field, and E is the local accelerating gradient.

Define structure parameters that also depend on wavelength:

$$s = \frac{E^2}{w}\ , \qquad z_s = \frac{E^2}{P_t} = \frac{s}{v_g}\ , \tag{2}$$

$$T_0 = \frac{2w}{p_d} = \frac{Q}{\pi f}\ , \qquad r = \frac{E^2}{p_d} = \frac{sT_0}{2}\ .$$

Here s is the elastance per unit length, z_s is the serial impedance, T_0 the attenuation time, p_d the power dissipated per unit length, and r is the shunt resistance per unit length. Multiplying by the appropriate power of wavelength yields the wavelength independent shunt reactance, serial impedance, and attenuation time are:

$$x_l \equiv \frac{s\lambda}{\omega} \equiv \frac{r}{Q}\lambda \equiv x_l\lambda \equiv \frac{s\lambda^2}{2\pi c}\ , \tag{3}$$

$$z_{sl} \equiv z_s\lambda^2, \quad T_\lambda \equiv \frac{T_0}{\lambda^{3/2}}\ .$$

For a zero aperture TM_{01} cavity, $x_l = 967T^2\ \Omega$, where T is the transit time factor. If the cavity is a half wavelength long it is 392 Ω. For the SLAC section middle cavity it is 440 Ω.

Values of these parameters as a function of a_λ, for a $2\pi/3$ mode disk-loaded structure with a disk thickness of 0.0556 λ, were obtained using the computer code TWAP.[1] These data are fit by expressions developed by the author and R. Palmer.[2] Either β_g or a_λ can be specified.

*Work supported by the Department of Energy, contract DE-AC03-76SF00515.

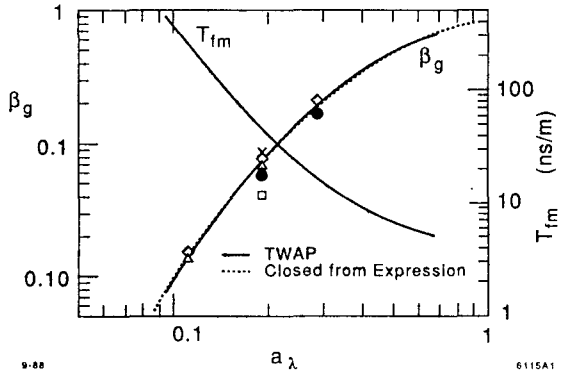

Fig. 1. Relative group velocity β_g and fill time per meter T_{fm} versus normalized aperture a_λ for $2\pi/3$ disk-loaded structure.

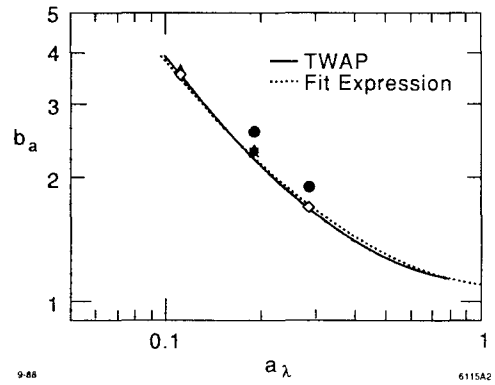

Fig. 2. Maximum radius to aperture radius ratio b_a versus normalized aperture a_λ for $2\pi/3$ disk-loaded structure.

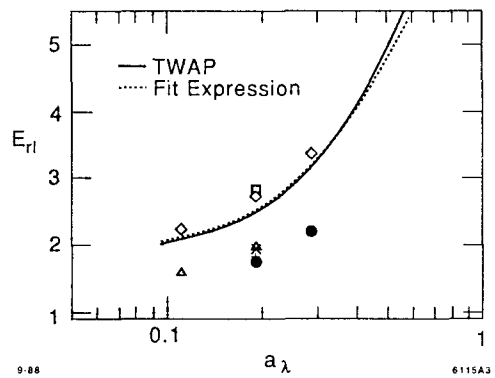

Fig. 3. Local peak to accelerating gradient ratio E_{rl} versus normalized aperture a_λ for $2\pi/3$ disk-loaded structure.

$$\beta_g = \exp\left\{3.1 - \frac{2.4}{\sqrt{a_\lambda}} - 0.9\,a_\lambda\right\}\ , \tag{4}$$

$$a_\lambda = \frac{0.31\,\beta_g^{1/4}}{(1-\beta_g)^{1/2}} + 0.3\,\beta_g\ .$$

$$b_a = 1.05\,\beta_g^{-0.28}\ , \qquad E_{rl} = 2 + 6\,\beta_g\ . \tag{5}$$

Contributed to the 1988 Linear Accelerator Conference (LINAC 88), Williamsburg, VA, October 3–7, 1988

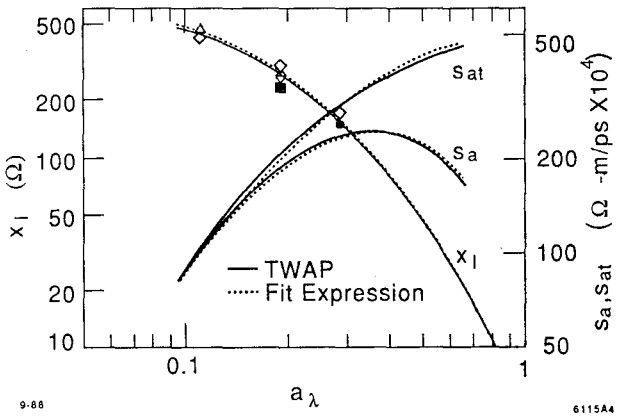

Fig. 4. Wavelength invariant elastance x_l and aperture invariant elastances s_a, s_{at} versus normalized aperture a_λ for $2\pi/3$ disk-loaded structure.

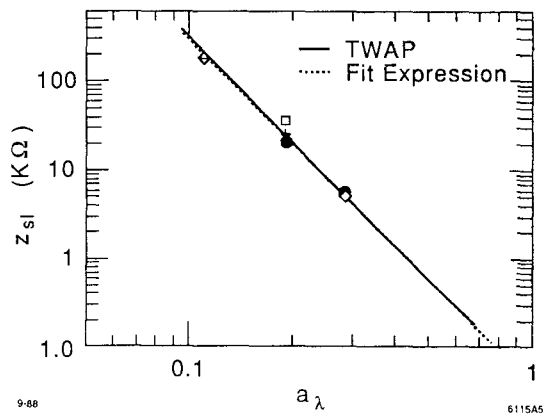

Fig. 5. Wavelength invariant serial impedance z_{sl} versus normalized aperture size a_λ for $2\pi/3$ disk-loaded structure.

$$x_l = \frac{30.24\,\beta_g^{0.4}(1-\beta_g)}{a_\lambda^2}, \qquad z_{sl} = 0.0413\,a_\lambda^{-3.836}, \tag{6}$$

$$T_\lambda = 45.5(1+1.25\,\beta_g^{3/2}) - 3\,\beta_g .$$

These expressions show proper asymptotic behavior as β_g approaches either zero or one.

The expressions for β_g, b_a, E_{rl}, x_l and s_{sl} versus a_λ are plotted in Figures 1 to 5. Also plotted in these figures are the points obtained directly from TWAP. These expressions have been plotted as function of relative group velocity.[3] The advantage of the plots here is that they can be compared with a large aperture SW structure and with π and zero mode cavities.

ACCELERATING SECTION PARAMETERS

The section parameters, the fill time, attenuation, efficiency and filling factor are:

$$T_f = \frac{L}{v_g}, \qquad \tau = \frac{T_f}{T_o}, \tag{7}$$

$$\eta_s = \frac{(1-e^{-\tau})^2}{\tau^2}, \qquad F_f \equiv 1-\beta_g .$$

Here, L is the section length. We can specify τ and L and obtain the wavelength and aperture from

$$\lambda = \left[\frac{T_f}{\tau T_\lambda}\right]^{2/3}, \qquad a = a_\lambda \lambda . \tag{8}$$

Define the section input serial impedance and section input elastance:

$$z_{ss} \equiv \eta_s z_s, \qquad s_s \equiv \eta_s s . \tag{9}$$

From Eq. (3) we obtain the local parameters at any frequency and aperture

$$s = \frac{x_l \omega}{\lambda} = \frac{x_l 2\pi c}{\lambda^2}, \quad z_s = \frac{z_{sl}}{\lambda^2}, \quad T_0 = T_\lambda \lambda^{3/2} . \tag{10}$$

The peak and average power inputs required to produce an average gradient E_a in a section[4]

$$P_p = \frac{E_a^2}{z_{ss}}, \quad P_a = \frac{f_r E_a^2 L F_f}{s_s} . \tag{11}$$

PEAK AND AVERAGE POWERS

Our choice of wavelength and aperture can be guided by plots of frequency, aperture, peak power and average power as a function of a_λ. Frequency and aperture vs a_λ for several combinations of τ and L are plotted in Figure 6. Peak and average powers per meter, for the same combinations of τ and L as in Figure 6, are plotted in Figure 7. (Because we are interested how much peak and average power is needed at a given gradient, it is more meaningful to plot the quantities $P_p/L = E_a^2/Lz_{ss}$ and $P_a/L = f_f E_a^2 F_f/s_s$ rather than z_{ss} and s_s.) These plots show how to trade increased frequency and decreased aperture for reduced peak and average powers. The fill time can be obtained from Figure 1.

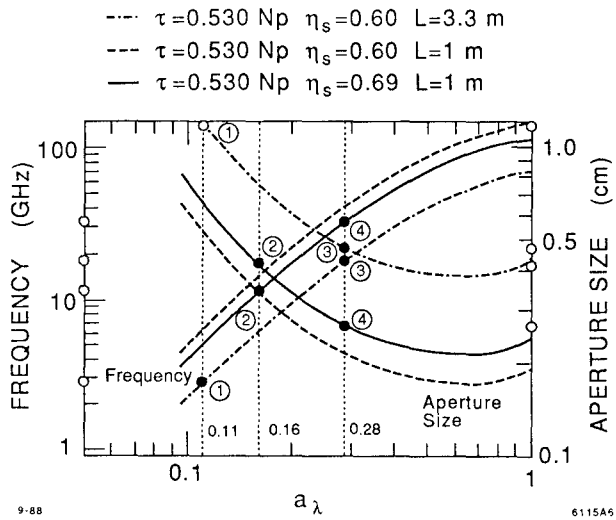

Fig. 6. Frequency and aperture size versus normalized aperture a_λ.

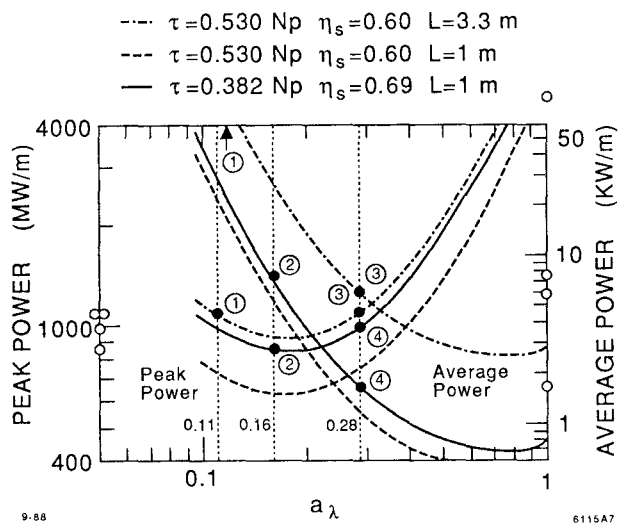

Fig. 7. Average and peak powers per meter versus normalized aperture a_λ with E_a = 200 MV/m and f_r = 120 Hz.

Table 1. LINAC DESIGNS

Frequency (MHz)	2856	11424	17320	30000
a (cm)	1.16	0.42	.484	0.28
b (cm)	4.06	1.03	.816	0.417
a/λ	0.11	0.16	0.28	0.28
β_g	0.0134	0.048	0.184	0.184
E_{rl}	2.10	2.3	3.1	3.1
T_0 (μs)	1.55	0.196	0.114	0.05
s (Ω/ps-m)	75	911	1009	3017
z_s (MΩ/m^2)	17.8	67.2	18.2	54.3
r (MΩ)	60	89	56	75
$x, r/Q$ (Ω/m)	4180	12692	9272	16000
L (m)	3.3	1	3.3	1
T_f (ns)	760	70	60	18
τ	0.53	.357	0.524	0.36
η_s	0.632	.707	0.60	0.705
E_a = 200 MV/m , f_r = 120 Hz				
P_p (MW)	3594	888	3620	1045
P_a (KW)	323	7.08	21.1	1.84
p_p (MW/m)	1089	888	1097	1045
p_a (KW/m)	98	7.08	6.4	1.84

Using Figures 6 and 7 as a guide, we choose the four designs of Table 1. The first is the 2.856 MHz benchmark design, the present SLC structure, except that here a constant impedance structure is assumed and the gradient is about 10 times the SLC gradient. Design 2 increases the frequency to 11.4 GHz and decreases the aperture to 0.42 cm. Consequently, the average power is reduced from 98 to 7 kW, the peak power remains essentially at 1 GW.

Design 3 increases the frequency to 17.3 GHz. It requires the same number of feeds as Design 1 (1/3 of Design 2). The peak and average powers per meter are about the same as for Design 2. The peak power per feed is the same as for SLC which at 20 MV/m gradient is 36 MW. The average power is reduced from 32 KW to 2 KW. Thus replacing the accelerator sections and the high power amplifiers, with that of Design 3, but keeping the same modulators with the same peak and average powers, would result in 16–fold increase in luminosity. The aperture is smaller, but a_λ is larger. Also, we may take advantage of the reduced b, from 4.06 cm to 0.82 cm, to place focusing coils along the accelerator sections.

Design 4 increases the frequency to 30 GHz. The peak power remains about the same, but the average power is reduced 50 fold. The peak powers are about the same for all four designs. The average power, however decreases sharply with decreased wavelength.

The dash curves in Figures 6 and 7 illustrate that increasing the section attenuation decreases both the peak and average powers at the expense of decreased wavelength and aperture.

OPERATION AT HIGH WAVELENGTH TO APERTURE RATIO

Increasing a_λ above 0.3 decreases the average power but it increases the peak power, even though the wavelength and aperture are both decreasing. This is desirable if high peak power is available, say by means of pulse compression. This can also be inferred from Figure 4, which shows that the aperture invariant elastance $s_a = sa^2$ has a maximum about $a_\lambda = 0.38$. This is the cutoff conditon for the TM_{01} mode in a circular waveguide with a radius to wavelength ratio a_λ. Thus, if at any aperture in the neighborhood of $a_\lambda = 0.38$, the elastance decreases as the frequency increases. As the TM_{11} beam breakup mode is at a higher frequency we expect that its elastance relative to the fundamental elastance is less than when we operate at lower a_λ. If $a_\lambda = 0.48$, the TM_{01} mode is attenuated at 26% below cutoff and the TM_{11} mode propagates at 26% above cutoff.

OTHER STRUCTURES

To determine whether we can do better than the bench-mark $2\pi/3$ disk-loaded guide, parameters for several additional structure shapes are plotted in Figures 1 to 5, superimposed on plots for the $2\pi/3$ structure. The structure shapes and the symbol used for plotting the parameters of each shape are shown in Figure 8. We note that their behavior with a_λ is similar to that of the disk-loaded guide and therefore they can be compared at any aperture, frequency, and section length. For the circular tip $2\pi/3$ mode at $a_\lambda = 0.11$, bench-mark design $E_{rl} = 2.1$. As a_λ increases to 0.19, E_{rl} increases to 2.5. If the tip changes from circular to elliptical, E_{rl} remains about the same. For the circular tip $\pi/2$ mode at $a_\lambda = 0.19$, $E_{rl} = 2.7$. Changing the tip from circular to elliptical reduces E_{rl} to 1.97. E_{rl} is less than the bench-mark value for the structure shapes shown in Figure 8, except for circular tip and the square-wall structures.

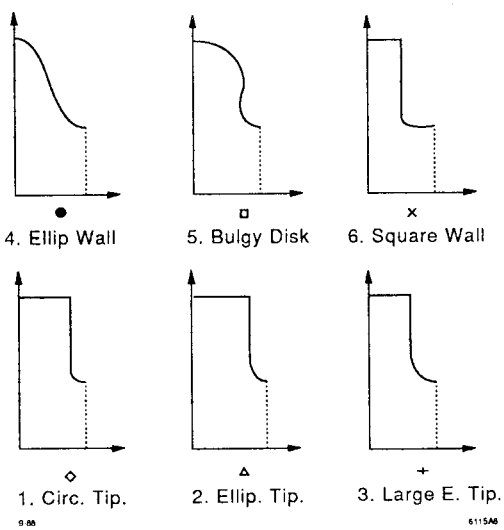

Fig. 8. Structure shapes.

As a_λ changes from 0.11 to 0.19, the resulting increase in b is a small fraction of the nearly two to one increase in a. The elastance is halved and the serial impedance decreases about nine-fold. This is, possibly, compensated by lowered wakefields, especially long-range wakefields. The elastance and attenuation time decrease for some shapes, and their use is indicated only if they result in ease of mechanical fabrication and lower wake fields.

ACKNOWLEDGMENTS

I am grateful to P. Wilson for his help and to R. Helm for his unstinting help in running his program TWAP.

REFERENCES

1. R. Helm, *"Computation of Properties of Traveling-Wave Linac Structures,"* SLAC-PUB-813, October 1970.
2. R. Palmer, *"The Interdependence of Parameters for TeV Linear Colliders,"* SLAC-PUB-4295, April 1987.
3. Z. D. Farkas, *"The Roles of Group Velocity, Frequency and Aperture in Traveling Wave Linear Accelerator Design,"* AAS Note 33, August 1987.
4. Z. D. Farkas, *"New Formulation for Linear Accelerator Design,"* IEEE Trans. of Nucl. Sci., **NS–32**, 2738 (1985).